Oxidation mechanism of thin Cu films A gateway towards the formation of single oxide phase

Sumita Choudhary, J.V.N. V N Sarma, Surojit Pande, S. Ababou-Girard, Pascal Turban, B. Lépine, Subhashis Gangopadhyay

Oxidation mechanism of thin Cu films: A gateway towards the formation of single oxide phase

Sumita Choudhary, J. V. N. Sarma, Surojit Pande, Soraya Ababou-Girard, Pascal Turban, Bruno Lepine, and Subhashis Gangopadhyay (iD)

View Online   **Export Citation**   **CrossMark**

ARTICLES YOU MAY BE INTERESTED IN

Oxidation mechanism of thin Cu films: A gateway towards the formation of single oxide phase

Sumita Choudhary,[1] J. V. N. Sarma,[1] Surojit Pande,[2] Soraya Ababou-Girard,[3] Pascal Turban,[3] Bruno Lepine,[3] and Subhashis Gangopadhyay[1,a]

[1]*Department of Physics, Birla Institute of Technology and Science, (BITS) Pilani, Rajasthan 333031, India*
[2]*Department of Chemistry, Birla Institute of Technology and Science, (BITS) Pilani, Rajasthan 333031, India*
[3]*IPR, UMR 6251, CNRS-Université de Rennes I, Campus de Beaulieu, 35042 Rennes, France*

Controlled thermal oxidations of thin copper films at relatively lower temperatures (up to 500°C) leading towards the formation of a single phase of copper oxide are investigated where the oxidation temperature, duration, oxygen partial pressure, film thickness and the crystallographic orientations play very crucial roles to significantly control the final phase of the copper oxide. Thin Cu films of thicknesses 100-1000 nm were deposited on glass and silicon substrates using the vacuum assisted thermal evaporation technique. Oxidations of those Cu films were performed at different temperatures for variable durations in air ambient as well as oxygen ambient conditions. Four probe resistivity measurement, x-ray diffraction (XRD), Raman spectroscopy, ultraviolet–visible (UV-Vis) spectroscopy, scanning electron microscopy (SEM) and x-ray photoemission spectroscopy (XPS) techniques have been used to characterize the oxide films. At a thermodynamic equilibrium, it has been observed that the oxide phase is solely determined by the oxidation temperature, however, the oxygen partial pressure can significantly alter this temperature range. In case of thermal oxidation in air, the initial oxidation of the copper films starts at about 150 °C, but a well ordered crystalline phase of the cuprous oxide (Cu_2O) is observed only above 200 °C. However, the cupric oxide (CuO) phase starts to appear only above 320 °C. The details of the oxidation mechanism of the Cu film are explained with a probable schematic model in terms of thermal diffusion as well as the chemical reactivity. © *2018 Author(s).*
All article content, except where otherwise noted, is licensed under a Creative Commons Attribution (CC BY) license (http://creativecommons.org/licenses/by/4.0/).
https://doi.org/10.1063/1.5028407

I. INTRODUCTION

Understanding of the oxidation process of metal thin films is of fundamental as well as high practical interest due to their environmental stability as well as for further processing of metal oxide based semiconductor nanostructures. From thermo-dynamical point of view, almost all the metals are having a tendency to be oxidized. The driving force behind the oxidation process of a given material depends on change in Gibbs free-energy due to oxide formation at that temperature. In general, thermal oxidation is a complex chemical process, where oxides are grown in an oxidant ambient at elevated temperatures. The simplest form of thermal oxidation of a metal surface may occur even at room temperature, when the film is exposed to an oxygen or air ambient and a thin layer of native oxide is formed. Afterwards, the oxide growth slows down and effectively stops within a few nanometers because of too little energy of the oxygen atoms to diffuse through the already formed native oxide layer at room temperature. However, thermal oxidation of metal films at an elevated temperature

[a]Corresponding Authors email: (subhagan@yahoo.com; subha@pilani.bits-pilani.ac.in)

may significantly be controlled by the oxygen atoms diffusion process and their chemical reactivity with the metal atoms. More precisely, the oxidation process is strongly influenced by the physical ambient such as temperature,[1] oxidant's partial pressure,[2] duration as well as the film thickness and their crystallographic orientations.

The exact oxidation kinetics of metals at nanometer scale also provides fascinating scientific information, which can be a demanding part of the rapidly growing field of nanoscience and nanotechnology. The controlled growth mechanism through surface processing may also lead to the formation of self-assembled ordered nanostructures of various shape, size and distribution (dots,[3] wires,[4] wells[5]), having very specific properties such as quantum confinements. Hence, controlled formation of oxide nanostructures would also be technologically very important for their potentially novel optical, electronic, magnetic and sensor properties. Therefore, surface oxidation may act as a processing tool for creating self-ordered semiconductor nanostructures, where a proper understanding of the oxidation mechanism will provide the essential insights into the complex growth kinetics of nanoscale oxide formation.

Transition metal oxides (TMO) are one of the most important classes of semiconductors[6] and have a wide range of applications in electronic devices and sensors as well as in the field of catalysts.[7] In addition, they are having significantly different properties at the nanometer length scale from their bulk materials.[8] Modern growth techniques also make it possible to grow various oxide nanostructures down to a nanometer scale. However, among the various TMOs, copper oxides attract much more attention due to their easy availability and non-toxicity with excellent electronic properties, which makes them very useful materials in the field of solar energy conversion, catalysis and gas sensors application.

In general, copper has two principal types of oxide: cuprous oxide (Cu_2O, cuprite) and cupric oxide (CuO, tenorite). Both oxides are p-type semiconductor in nature but have different physical, chemical and electronic properties such as colour, crystal structure, band gap etc., which lead them to specific applications towards devices, sensors and catalysts. More precisely, Cu_2O shows a cubic structure ($a = 4.27$ Å) and exhibits a direct band gap of ~2.1eV.[9] As the band gap is lying in the visible light wavelength range, Cu_2O thin films can be used as an absorber layer in solar cells,[10–12] cathode material for micro batteries[13] and material for photo-catalytic degradation of the organic pollutants towards solving the environmental problems related to water splitting and anti microbial applications.[14] Moreover, its outstanding excitonic properties including a large exciton binding energy (~140 MeV) have also attracted many fundamental researches.[15] On the other hand, CuO appears in monoclinic structure ($a = 0.4684$ nm, $b = 0.3423$ nm, $c = 0.5128$ nm and $\beta = 99.54°$) with an indirect bandgap in the range of 1.21 - 1.50 eV.[16] This material has potential use in the field of gas sensor applications,[17,18] along with magnetic storage media,[19] solar energy transformation,[20] varistors and catalysis as well.[21]

Although, there are several reports on the exploitation of Cu_2O as an active layer for solar cells, the conversion efficiencies of them are still much lower (~2%) as compared to its theoretical value of around 20%.[10,22] It is often claimed that the low open-circuit voltages resulting from rapid interfacial carrier recombination are responsible for it. In addition, the gain and heat losses of the solar cell may also depend on the oxide phase purity, optical properties and crystalline quality of the Cu_2O material. Hence, to prepare single oxide phase of copper films with high crystalline quality is of high practical demand to further investigate its electronic properties. It has also been reported that the photo-catalytic performance of Cu oxides is very much limited by the recombination of the photo-excited electrons and holes.[23] All these phenomena make the phase purity of the copper oxides an important issue which demands further attention of the research community.

Various growth techniques have been employed for device quality copper oxides formation such as, sol-gel process,[24] spray pyrolysis,[25] solution growth,[26] chemical vapour deposition (CVD),[27] pulsed laser deposition (PLD)[28] and DC and RF magnetron sputtering,[29–32] molecular beam epitaxy (MBE),[33] anodic and chemical oxidations,[34,35] and electrochemical deposition.[36–38] These growth techniques generally require some special growth conditions, however, still results in a mixed oxide phases. Hence, formation of a single oxide phase of Cu thin films is of high practical importance for photovoltaic devices and sensor applications.

As most of the cases chemical growth routes were followed where the material purity is a critical issue due to the possible unintentional contamination. However, vacuum assisted growth of oxide material under cleaner ambient through physical route would be an alternative approach.[39–44] Valladares *et. al* reported the oxidation of thin Cu films under air annealing where an increase in electrical resistivity of the films due to oxidation has been observed.[39] Derin et al. reported the optical properties of the Cu oxide film grown by thermal annealing of Cu films.[40] Ellipsometry was used in the visible region to determine the Cu_2O film thickness by measuring the optical constants *n* (refractive index) and *k* (extinction coefficient). In addition, band gap of the oxide films was also measured from the absorption spectra. They observed a linear time law for Cu_2O growth and band gap of about 2 eV. Papadimitropoulos et al. have also reported the formation of copper oxides by thermal annealing where they found an optical band gap of about 1.1eV and 2.3 eV for CuO and Cu_2O, respectively.[41] Musa *et. al* reported the formation of a mixed oxide phase of Cu between 200 °C and 1040 °C whereas a single oxide phase of Cu_2O is grown at a temperature of 1050 °C.[42] Figueiredo and co-worker found a drastic increase in the optical transmitivity of the copper oxide film after annealing at a temperature above 200 °C and a variation of band gap between 2-3 eV.[43]

Although several works on thermal oxidation of Cu films have already been reported, a systematic study of the oxidation mechanism and temperature dependent diffusion process of the oxidizing species leading towards the oxide phase transition at lower oxidation temperature is still lacking. In this paper, a simple and efficient approach, vacuum assisted evaporation of thin metal films followed by controlled thermal oxidation (up to 450 °C) has been used to form a single phase of copper oxides.

II. EXPERIMENTAL DETAILS

Thin copper films of various thicknesses were deposited at room temperature on glass and silicon substrates, using the vacuum assisted thermal evaporation technique. All substrates were ultrasonically cleaned with acetone, isopropanol, and methanol for about 15 minutes followed by drying with pure nitrogen gas, prior to loading into the vacuum chamber. During Cu deposition, the chamber pressure remained in the range of $\sim 10^{-5}$ mbar and the evaporation rate was maintained about ~ 3 Å/sec to have uniform and homogeneous films. The as-grown copper films were then thermally oxidized in air as well as oxygen ambient at various temperatures for different durations. The oxidation temperatures were varied in a wide range from room temperature (RT) to 450 °C in a precisely controlled manner. A slow cooling rate of < 10 °C/min was preferred to minimize the possible thermal stress and improve the crystalline quality of the oxide films.

All copper oxides films were characterized for structural, morphological, optical, chemical and electrical properties using various analytical techniques. To investigate the initial oxidation of Cu films, sheet resistance of the thin Cu films was measured by the four point probes technique with a probe-spacing of 4 mm, using the Physical Quantity Measurement System (PQMS) from Qazartech. The crystallographic structures of the oxide films were investigated by Rigaku Mini Flux II X-ray diffractometer (XRD). Cu-Kα radiation ($\lambda = 1.54$ Å) was used as X-ray source with an accelerating potential of 30 kV for emission current of 15 mA. The surface morphology of the copper oxide films was analyzed with a commercial field emission scanning electron microscopy (FESEM) from Nova NanoSem 450, operated from 0.5 to 30 kV. Optical transmittance of the oxide films was recorded using a Simazu UV-visible optical spectroscopy within the wavelength range of 300–800 nm and the optical band gap of the oxide films are estimated. Raman spectroscopy measurements were also performed to distinguish the oxide phases of the films, using a commercial Raman unit from Horiba Scientific. Finally, X-ray photoemission spectroscopy (XPS) measurement was performed to find the oxidation states of Cu and the phase purity of the copper oxides layer. During XPS measurements, the base pressure of the chamber was maintained below < 10^{-9} mBar and monochromatic Al K$_\alpha$ (1486.6 eV) and Mg K$_\alpha$ (1256.7 eV) lines were used as X-ray sources. All binding energies of the emitted photoelectrons are calibrated to the C1s line positioned at 284.5 eV of the contaminant from the ambient.

III. RESULTS AND DISCUSSION

A. Oxidation of Cu films: Effect of temperature

1. Initial oxidation

Four probe resistivity measurement technique has been employed here to find the temperature required for the initial oxidation process of the Cu films. To measure the sheet resistance (R) of the Cu films, outer two probes were used as current (I) source whereas the inner two were used to measure the voltage drop (V) across the surface. The samples were annealed in air as well as helium ambient within a metal tube, equipped with a cylindrical heater. A silicon diode was used to measure the sample temperature (uncertainty of ±10 °C). It is important to mention that the annealing temperature rises almost linearly with a heating rate of 2 °C/min from room temperature up to 130 °C. Afterwards, the heating rate becomes much slower and the rate was observed to be 0.15 °C/min during the last 5 °C of annealing. In Figure 1, temperature dependent sheet resistance of the Cu films in air ambient are depicted where the increase in sheet resistance (R) with the annealing temperature (T) is shown. A linear increase in resistance with annealing temperature (T) has been observed for temperature up to 140 °C. This constant slope of the R-T plot can be related to the thermal coefficient of resistivity of the Cu film. However, a sudden increase/jump in sheet resistance is observed above 140 °C, which indicates the onset of surface oxidation of the Cu film at this particular temperature.

For further confirmation of the initial surface oxidation process of Cu film during annealing above 140 °C, R-T measurements with heating and cooling cycle have been performed on a Cu film initially in a helium ambient followed by in an air ambient. Both R-T plots with heating and cooling cycles are depicted within the inset (a) of Figure 1. In case of He ambient annealing, the R-T plot linearly increases up to 150 °C without any sudden jump/increase in sheet resistance. In addition, the cooling cycle almost follows the heating path indicating no such chemical changes (oxidation) of the film surface during annealing under He ambient condition. Whereas, for air ambient annealing, same sample shows a rapid increase in sheet resistance just above 140 °C. Moreover, the cooing path follows the heating slope but with a constant upward shift due the oxide layer formation above 140 °C.

To avoid any kind of uncertainty, the resistivity measurements of the heating and cooling cycles have also been performed in air for Cu films of different thickness, as can be seen within the inset (b) of Figure 1. To have better statistics and minimize any kind of contact errors, all I-V data was recorded at a particular temperature and the corresponding slope was then measured to plot the R-T data here. The linear increase in resistance with annealing temperature having a constant slope related to the thermal coefficient of resistivity is also followed. Both the heating and cooling lines show almost identical slopes. In addition, a minor vertical shift in sheet resistance for the cooling line as compared

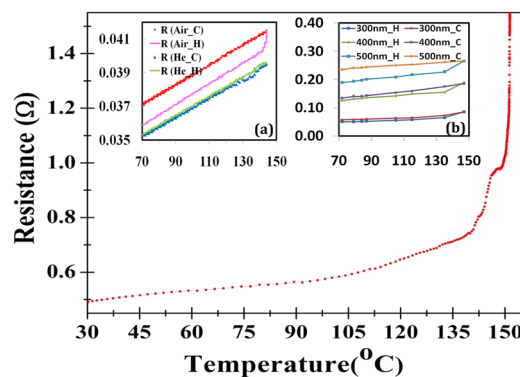

FIG. 1. Temperature dependent sheet resistance of Cu films during annealing in air. Insets show the R-T measurements of heating and cooling cycles. Comparison of sheet resistance: (a) during He and air ambient annealing (b) of different film thicknesses during air annealing.

to that of the heating is recorded in each film. This could due to be the fact that the oxide layer formation starts on Cu surface above 140 °C, during annealing in air ambient condition.

From all the above findings we can conclude that thermal oxidation of the copper film in air starts at about 150 °C which can be explained in the following way. Spontaneous formation of a very thin native oxide layer on copper film is quite obvious at room temperature as soon as it is exposed to air. Afterwards, this native oxide layer acts as a barrier for further oxidation of the Cu film by limiting the diffusion of the oxygen molecules through it. As a result, further oxidation of the Cu film is protected at room temperature. However, at about 150 °C, thermal energy starts to overcome the diffusion barrier and further oxidation of Cu film starts, which is clearly reflected by a sudden increase in the slope of the R-T plot. A vertical shift in sheet resistance from heating to cooling cycle within the R-T plot also indicates an increase of the sheet resistance by slight thickening of the oxide layer during annealing of the film above 140 °C. As the heating rate was quite slow at this temperature range and altogether the duration of annealing above 140 °C was more than 30 min, a reasonable amount of surface oxidation may be expected, which further reflects the change in the sheet resistance. A similar jump in bulk resistivity for Cu film has also been reported by Valladares *et. al.* after air oxidation.[39]

2. Temperature dependent oxide phases

In order to understand the formation of various copper oxide phases, XRD analysis of thin copper films has been performed as a function of oxidation temperature (Figure 2). All films were furnace annealed within a closed chamber in air ambient at different temperatures and durations. As-deposited Cu films show sharp diffraction peaks centered at about at 43.4° and 50.6° (2θ value), attributed to the (111) and (200) reflection planes, respectively (Fig. 2(a)).[39,43] Sharp diffraction lines confirm the formation of a well oriented and crystalline Cu film on glass substrate, even after Cu deposition at room temperature. As compared to the reported chemical growth process, the pattern shows only two or three diffraction lines which are also an indication of a preferential growth orientation of the Cu film. Although, earlier sheet resistivity measurements suggest that the oxidation process of the Cu film in air starts at about 150 °C, we have not observed any XRD peaks of copper oxides below 250 °C. [This ambiguity will be discussed later in Section III C 1 with the help of Raman spectroscopy as well as XPS]. Figure 2(b) shows the XRD patterns start to change only after oxidizing the film at a temperature above 250 °C. In addition to the Cu diffraction lines, an additional diffraction peak centered at 2θ = 36.4° starts to appear. This peak position represents an inter-planar lattice spacing of d = 2.44 Å which can be attributed to the (111) reflection planes of cubic phase Cu_2O [JCPDS card no.: 05-667, 31, 35]. Figure 2(b) represents the XRD patterns of Cu films annealed at 280 °C for 3 hours which appears with a new diffraction peak at 2θ = 36.4°. This can be concluded as the initial stage of crystalline Cu_2O phase formation and as a whole, the film exhibits a mixture of Cu and
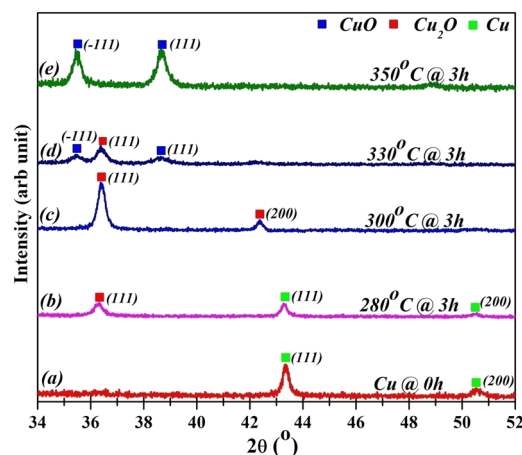

FIG. 2. XRD spectra of thin Cu films after oxidation in air at various temperatures for different durations.

Cu_2O phases. Continuation of the oxidation process at the same temperature will result in an increase of the Cu_2O (111) diffraction peak intensity whereas a decrease in the Cu diffraction peaks and finally the hole Cu film will convert into a crystalline Cu_2O phase, with a strong preferential orientation along (111) lattice plane. Towards the end of the oxidation process, a weak diffraction peak centered at 42.3°, corresponding to Cu_2O (200) starts to appear.[39,43] Further increasing the oxidation temperature does not change the scenario very much except a faster oxidation process. Figure 2(c) shows the XRD pattern, after oxidation at 300°C for 3 hours where the additional diffraction peak of Cu_2O (200) has become much stronger. However, we have not seen any trace of CuO formation at this temperature. It has to be taken into account that XRD in not a very surface sensitive techniques and it may only detect an oxide phase after a significant amount of surface oxidation of the Cu film (∼5%) has already been occurred. However, prolonged oxidation (up to 20 hours) at a temperature below 320 °C does not show any trace of CuO formation in XRD pattern which successfully excludes the formation of CuO at this temperature.

A drastic change in XRD pattern is only found for oxidation above 320 °C, as an indication of CuO formation. Two low intensity diffraction peaks centered at $2\theta = 35.5°$ and 38.8° start to appear on either sides of the Cu_2O (111) peak (Fig. 2(d)). These diffraction lines can be attributed to the (−111) and (111) reflection planes, respectively, of the CuO monoclinic phase [JCPDS cards no.: 45-0937, 39, 43]. The film predominantly consists of Cu_2O phase along with a small amount of CuO phase. Continuation of oxidation at this temperature slowly converts the whole film into a crystalline CuO layer at the cost of Cu_2O phase. Further increase in oxidation temperature results in a faster oxidation of the film to CuO, as shown in Fig. 2(e) [350 °C for 3 hours].

From all these above findings it can be concluded that the oxide phase of the Cu film is strictly determined by the oxidation temperature, which can be explained in terms of chemical activation energy of the oxide phase formation. Gibb's free energy change (ΔG) for chemical reaction is determined by the changes in enthalpy (ΔH), entropy (ΔS) and the absolute temperature (T) as:

$$\Delta G = \Delta H - T(\Delta S)$$

where, an increase in absolute temperature T results in a decrease in the ΔG value. A reaction can be spontaneous only if the value of the free energy (ΔG) becomes negative. Hence, the onset of native oxide (Cu_2O) formation at room temperature, during exposure of the Cu film to air, indicates that the value of ΔG is negative for Cu_2O formation. However, the oxidation process was mainly restricted by the diffusion kinetics of the O_2 through the surface oxide layer. With increase in temperature, thermal energy helps to overcome the diffusion barrier as oxidation proceeds. But there was no trace of CuO formation below 320 °C, even for a long duration (20 hours) of oxidation as the diffusion kinetics does not play any significant role here. Therefore, it is expected that at lower temperature the value of ΔG is to be positive in case of CuO formation, which turns to a negative value when the temperature exceeds 320 °C and as a result it overcome the chemical reaction barrier. Moreover, even after oxidation for sufficiently long duration (*i.e.* under thermodynamic equilibrium) we have not seen any coexistence of CuO with the metallic Cu phases. This finding also confirms that at thermodynamic equilibrium oxide phase is solely determined by the oxidation temperature, not by the growth kinetics. Finally, for both Cu oxides, increase in temperature enhances the diffusion kinetics of the O_2 and as a result a faster oxidation occurs. Therefore, it can be concluded that at thermodynamic equilibrium copper oxide formation by thermal oxidation follows the phase sequence of Cu → (Cu + Cu_2O) → Cu_2O → (Cu_2O + CuO) → CuO, where pure Cu_2O phase occurs for a small window of annealing temperature between 250 °C and 320 °C. A similar kind of copper oxide phase evolution with oxidation temperature has also been reported.[39,41,43]

However, the above theory can only explain the oxide growth at elevated temperature as it does not include any terminal cases of oxidation process at room temperature as well as higher oxidation temperature. Here, we will explain the terminal cases of oxidation process in terms of chemical activation energy as well as thermal diffusion of O_2 and Cu species. In one hand, the oxidation of Cu films at room temperature terminates within the native oxide layer of few nanometers thickness which can be explained in the following manner. The native oxide layer acts as a diffusion barrier for O_2 and Cu species at room temperature and plays a preventive role against any further oxidation of Cu film and by restricting the diffusion process. In addition, limited chemical activation energy

at room temperature also restricts the further Cu$_2$O growth in this *reaction-limited* growth regime. As the oxidation temperature increased, diffusion energy also increases and starts to overcome the native oxide barrier at about 150 °C. As a result, further oxidation of the Cu film continues. On other hand, oxidation of Cu films at elevated temperature also terminates to its saturation thickness with a thick oxide layer. As the oxide layer gets thicker it drastically reduces the diffusion process of O$_2$ and Cu species. As a result, oxide growth rate slows down significantly in this *diffusion-limited* growth regime and finally terminates. Therefore, the final oxide layer thickness limits to the saturation thickness which is mostly determined by the oxidation temperature not by the duration of oxidation.

B. Diffusion kinetics

Within the limit of chemical activation energy, temperature induced thermal diffusion process of O$_2$ molecules leading towards the change of oxide phase (Cu→Cu$_2$O and Cu$_2$O→CuO) are discussed in this section. XRD intensity profiles are intensively used here for quantitative analysis of the oxide growth as a function of oxidation time. Starting from the metallic Cu films, their stepwise oxidations at 260 °C and 300 °C up to the completion of Cu$_2$O phase, depends on the duration of oxidation as depicted in Figures 3(a) and 3(b), respectively. The XRD patterns of the initial Cu film appear with strong diffraction peak at 2θ = 43.4°, originating from the Cu (111) reflection planes. With duration, the oxide phase starts to become visible at 2θ = 36.4°, representing the (111) lattice planes of

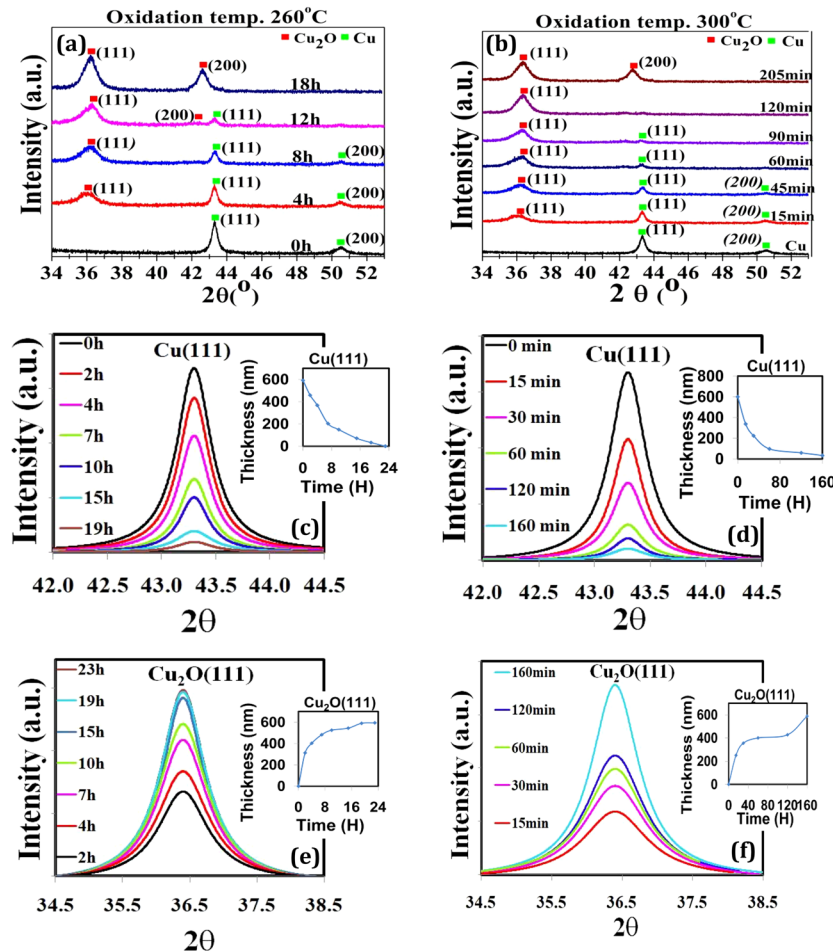FIG. 3. XRD spectra of thin Cu films during evolution of Cu$_2$O oxide phases after oxidation in air at (a) 260°C and (b) 300°C, for different durations. Lorentzian peak fitting of (c-d) Cu(111) and (e-f) Cu2O (111) diffraction lines, along with their oxide growth kinetics shown within the insets.

Cu_2O phase. This peak gets stronger at the cost of Cu (111) peak intensity, following domination over the metallic Cu phase, and finally completes to the pure Cu_2O phase. Moreover, an additional diffraction peak at $2\theta = 42.3°$ attributed to the (200) reflection planes of Cu_2O has also been observed towards the completion of the oxide phase. However, it is quite clear from the comparison of both the XRD patterns that the Cu_2O oxidation process is much faster at 300 °C as compared to that of 260 °C. A quantitative analysis of the oxide growth at 260 °C and 300 °C, as a function of oxidation time, is depicted in Figures 3(c)–3(f). To determine the amount of remaining metallic Cu as well as the amount of Cu_2O grown through surface oxidation process, a Lorentzian profile has been fitted to the data of the Cu (11) and Cu_2O (111) peaks and displayed in Figs. 3(c) and 3(d) and Figs. 3(e) and 3(f), respectively. A gradual decrease in Cu (111) peak intensities as well as a gentle increase in Cu_2O (111) peak intensities with the oxidation timing are clearly depicted in Figs. 3(c) and 3(d) and Figs. 3(e) and 3(f), respectively. Assuming a homogeneous lateral growth of Cu_2O through the surface diffusion of O_2, an estimated depth profile of Cu or Cu_2O are also summarized within the inset of each intensity diagram. Here, we assume a uniform and homogeneous oxidation for all crystallographic orientations which may not be case for the actual oxidation process. The effect of crystallographic orientation on the oxidation process is briefly discussed later in the Section III G. In general, the oxide growth profiles (presented within the insets) follow an overall parabolic pathway with the duration of oxidation. On the other hand, the Cu (111) peak intensity shows a similar similar decay with the oxidation time. A careful observation of the oxide growth profiles also suggests that the oxide growth rate is much higher at the initial stage and then slows down with layer thickness and finally terminates. Moreover, a relatively broader diffraction peaks for Cu_2O as compared to metallic Cu can also be noticed.

The impact of further oxidation of Cu_2O films to CuO layer at temperatures of 330 °C and 350 °C, is shown in Figure 4. In this case, two diffraction peaks centered at $2\theta = 35.5°$ and 38.8°, attributed to the (-111) and (111) diffraction lines of CuO, appear after the first annealing step. With duration, both peaks strengthen at the cost of Cu_2O diffraction lines. Moreover, a relatively broad defection peak is found for CuO in comparison to Cu_2O. The average crystalline size of the oxide grains may be calculated using the Debye-Scherer formula:

$$D = (0.91\,\lambda) \,/\, (\beta\,Cos\theta)$$

where 'λ' is wavelength of X-ray (Cu K_α: 1.541Å), 'β' is full width half maximum (FWHM) peak, 'θ' is diffraction angle and 'D' is particle diameter size.[45] A gradual decrease in crystallite grain size starting from Cu $\rightarrow$ Cu_2O $\rightarrow$ CuO has been found. The average grain sizes of (111) plane for Cu, Cu_2O and CuO are found to be 41, 24 and 16 nm, respectively, where the Cu_2O and CuO layers were formed by oxidation at 320 ºC for 9 hours and 350 ºC for 3 hours, respectively.

Within the phase equilibrium, faster oxidation at higher temperature can be explained in following ways. In case of Cu_2O formation, both the oxidation temperatures 260 °C and 300 °C are kept below the activation energy for CuO formation (330 °C) whereas for CuO formation oxidation temperatures are set well above the critical temperature of 325 °C. Hence, for both the cases, O_2 diffusion mechanism plays the key role rather than thermodynamics. An increase in oxidation temperature can drastically enhance the O_2 diffusion process through the oxide layer. Hence, a faster growth of Cu_2O layer at 300 °C as compare to 260 °C as well as rapid CuO growth at 350 °C as compare to 330 °C is quite obvious due to an enhanced diffusion of oxidizing species.

The thickness dependent Cu_2O growth rate shown within the insets can be correlated to the following matter. At an early stage of oxidation the oxide layer is relatively thin. As a result, time taken by the oxidizing species to reach the Cu_2O/Cu interface through diffusion process is much faster than the timescale needed for the chemical reaction to form the Cu_2O. A faster growth rate of oxide film at this initial phase is expected which can be assigned as the *reaction-limited* growth regime. On the other hand, when the oxide layer becomes thicker, the timescale of diffusion through this layer exceeds the reaction timescale. Therefore, at the later stage the oxidation rate becomes slower and it is assigned as *diffusion-limited* growth regime. More detailed analysis of the diffusion process is discussed in the following.

Diffusive flux (F_1) of the oxidizing species through the Cu_2O over layer to Cu-Cu_2O interface can be represented as $F_1 = D\,(dC/dx) \cong D\,(C_0−Cs)$, where C_0 is the concentration of the oxidizing
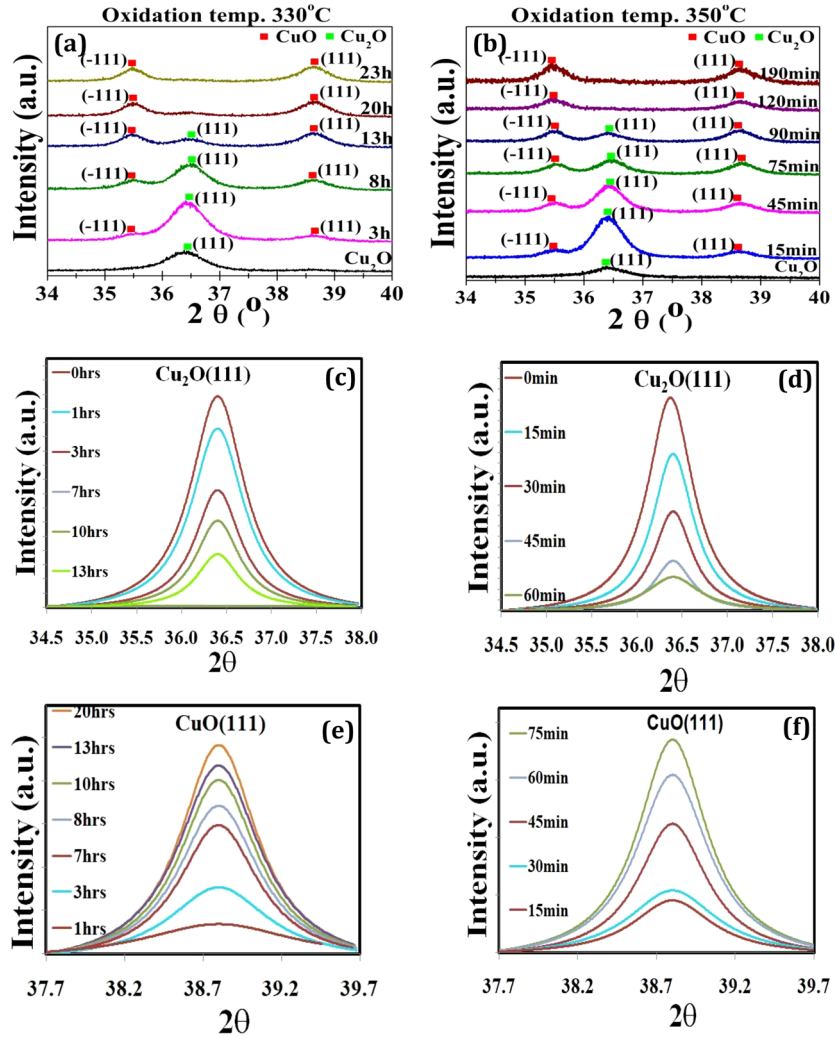
FIG. 4. XRD spectra of thin Cu_2O films transformation to CuO oxide phases during thermal oxidation in air at (a) 330°C and (b) 350°C, for different durations. Lorentzian peak fitting of (c-d) $Cu_2O(111)$ and (e-f) CuO (111) diffraction lines.

species in atmosphere adjacent to the film surface, C_s is the concentration of the oxidizing species at the Cu-Cu_2O interface, D is the diffusion coefficient of the oxidizing species, and x is the thickness of the oxide layer. As the reaction rate of the oxidizing species is proportional to C_s, the reactive flux (F_2) can be represented as $F_2 = kCs$, where k is the reaction rate. In case of initial oxidation within the *reaction limited regime*, the oxidation rate is mainly controlled by the flux rate F_2, whereas for thicker layer of oxide in *diffusion limited regime*, F_1 is the deciding factor of the oxide growth rate. However, in both regimes F_1 and F_2 becomes equal (F) for a steady-state of oxidation and can be represented as $F = DC_0 (x+D/k)$, which gives the growth rate of the oxide layer as $dx/dt = Dk (C_0/C_1)/(kx + D)$, and C_1 represents the number of oxidizing species per unit oxide volume. The differential equation, with the initial condition of $x(t = 0) = 0$ yields a generalized quadratic equation:

$$x^2 + Ax\text{-}Bt = 0,$$

where, $A = 2Dk$ and $B = 2DC_0/C_1$. Our findings of a parabolic pathway of oxide layer growth with the oxidation time are very much in line with this generalized equation. A very similar kind of oxidation mechanism has also been reported by Dale *et al* for oxidation of silicon surface.[46] However, the minor variation in experimental data may be related to the non-uniform oxidation for the different crystallographic planes.

C. Optical properties

1. Oxide phases

To identify the various oxide phases of the copper film, apart from the XRD analysis discussed earlier, Raman spectroscopy has also used as a probing technique, as shown in Figure 5. The room temperature Raman spectroscopy measurements of the thin oxide films are performed within the spectral region of 50 - 900 cm^{-1}. Figure 6 represents the micro-Raman spectroscopy of thin Cu, Cu$_2$O (annealed at 300 °C for 3h), mixed oxide (Cu$_2$O + CuO) and CuO (annealed at 350 °C for 3h) films. A typical Raman spectra obtained from nanocrystalline Cu$_2$O thin films exhibits two strong peaks at 217 cm^{-1} and 146 cm^{-1} correspond to the Cu$_2$O oxide phase.[46,47] In case of CuO, three peaks centered at 292, 341 and 626 cm^{-1} are observed, which can be identified as the first order A$_g$ and 2B$_g$ phonon scattering.[47,48] For thin films of mixed oxide phases Raman spectra show a combination of both set of peaks assigned to Cu$_2$O and CuO. In general, the Raman spectroscopy results are in good agreement with our XRD findings and reveal a similar kind of phase transformation of the Cu$_2$O to CuO during oxidation at a temperature above 320 °C. However, oxidation of the Cu films at a lower temperature, between 150 °C to 250 °C, Raman data reveals very different information in
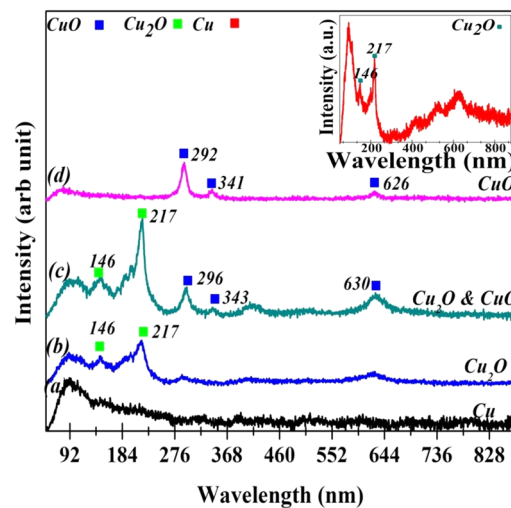

FIG. 5. Raman spectra of various Cu oxides films grown by thermal oxidation of thin Cu films in air. Inset shows the Raman spectrum of Cu film oxidized at 220°C for 4 hours in air.
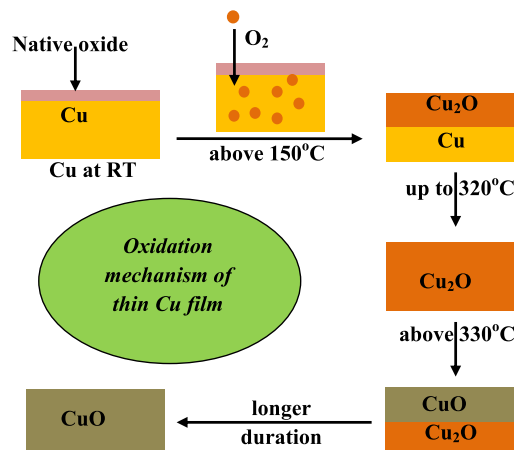

FIG. 6. Oxide growth schematics of thin Cu film during thermal oxidation in air.

contrast to our earlier XRD findings. A clear existence of Raman peaks at 146 cm^{-1} and 217 cm^{-1} is observed after oxidation of a Cu film at 220 °C for 4 hours, which clearly indicates the presence of Cu_2O phase [inset of Fig. 5]. Whereas, XRD result does not show any trace of Cu_2O (111) reflection peak and appears only with the Cu diffraction lines. Thus, based on the Raman and the XRD analysis, it can be concluded that both Cu and Cu_2O phases coexist within the oxidized films. This finding is also consistent with our four probe resistivity measurement where the oxide formation of the Cu film is predicted above 150 °C. XRD analysis could not detect the presence of Cu_2O due to the following reason. As a fact, XRD can only detect crystalline grains of sufficient size of the oxide material, whereas Raman technique is capable of detecting the amorphous states too. In addition, Raman spectroscopy is much more surface sensitive as compared to the XRD. Since the Cu_2O phase starts to form through surface oxidation, it would be easier with Raman spectroscopy to detect even for a very thin over-layer of oxide on Cu film rather than the XRD can detect only after a significant amount of surface oxidation. A similar kind of discrepancy has also been reported by other researchers.[47] Therefore, the ambiguity we mentioned earlier (Section III A 2) can be solved in the following manner: Oxidation of the Cu films below 250°C results in a mixed phase of Cu and Cu_2O. Either the oxide layer is very thin or all the grains are very small (poor crystalline state). These assumptions are well justified by a very limited thermal diffusion of oxidizing species and Cu atoms at lower oxidation temperature. As discussed earlier, native oxide layer acts here as a diffusion barrier and with increase in annealing temperature diffusion above 150 °C, thermal energy starts to overcome the barrier and oxidation continues. However, the diffusion process at this temperature still remains very much limited which may result in a poor crystalline state of the Cu2O layer. As the ambiguity of the 4-probe resistivity and the XRD measurements is solved, for a better understanding of thermal oxidation mechanism, we introduce here a schematic of the surface oxidation process of thin copper films and the effect of oxidation temperature, as shown in Figure 6. Exposure of a fresh copper film to air ambient results in a spontaneous native oxide formation, which later acts as a diffusion barrier for O_2 and prevents the further oxidation. The thermal energy at 150 °C, overcomes the diffusion barrier and Cu_2O formation starts. However, activation energy of CuO formation demands a higher thermal energy (325 °C). In all cases, a longer duration of oxidation results in a thicker oxide layer whereas the oxidation temperature determines the oxide phase.

2. Optical band gap

To further identify the oxide phase of the Cu thin films oxidized below 320 °C and determine the optical band gap of the Cu_2O film, UV-visible spectroscopy is employed. Figure 7 shows the optical transmission spectra of Cu_2O thin films of different thicknesses. In addition, the absorption coefficient (α) is also plotted against the photon energy (E_g) to estimate the optical band gap of
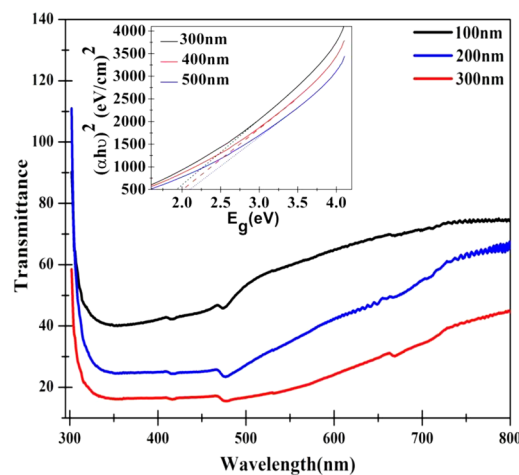

FIG. 7. UV-visible spectra of Cu_2O thin films grown by thermal oxidation in air ambient. Inset shows the optical band gap for different Cu_2O film thicknesses.

thin Cu_2O films (inset of Fig. 7). The absorption coefficient (α) is determined with the help of "Kubelka - Munk formula":

$$F(R) = (1\text{-}R)^2 / 2R$$

where, R is the reflectance, and F(R) is proportional to the absorption coefficient (α).[49] The photon energy is calculated by using hc/λ, where h represents the Planck's constant and λ is the wavelength in nm. Finally, the optical band gap is estimated by linear extrapolation, as can be seen within the inset of Fig. 7. The result shows a direct band gap of nearly 2.1 - 2.3 eV, which lies in the visible light range and also suggests a single oxide phase of Cu_2O thin films.[9,41]

D. Oxide surface morphology

To investigate the surface morphology of the thin copper films oxidized at different temperatures, scanning electron microscopy is used as a characterizing tool here. It is found that the surface morphology of the thin Cu film is very much dependent on its growth parameters and the choice of the substrate. But, the surface morphology of the oxide films can highly be influenced by its materialistic property of the oxidation state of copper film rather than the growth mechanism (temperature, film
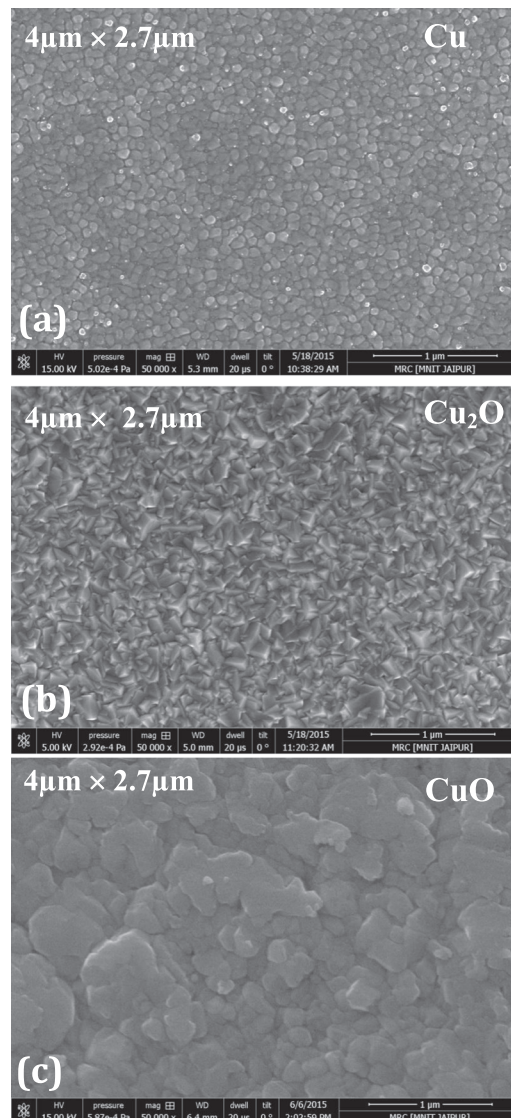

FIG. 8.   SEM image of 400 nm thick Cu films on glass substrate: (a) as-grown (b) oxidized at 300°C and (c) 350°C, respectively.

thickness, duration). Figure 8 shows field emission scanning electron microscope (FESEM) images of 400 nm thin Cu films oxidized at different temperatures for 4 hours. The as-grown Cu film surface shows a smooth morphology and appears with uniformly distributed homogeneous clusters of 60-80 nm lateral size (Fig. 8(a)). However, the Cu_2O film surface appears with a very different surface morphology with highly faceted structures consisting of tetrahedron shaped islands which can clearly be seen after oxidation at 300°C (Fig. 8(b)). This faceted morphology is very much related to the structural characteristic of the cuprous oxide.[50] Fig. 8(c) depicts the surface morphology of a CuO film oxidized at 400 °C for 4 hours. A relatively rough surface morphology with in homogeneously grown granular layered structures is found. Transition of the faceted Cu_2O structures into a rough granular surface morphology may be related to the transition of cubic Cu_2O to monoclinic CuO layer. However, oxidation at even higher temperature results in faceted CuO nanostructures with larger crystallite size where higher thermal mobility results in an improved crystalline phase as well as the coalescence of the smaller grains into a larger grain.[47]

E. Chemical properties and oxidation states

In order to further investigate the oxide phase purity, i.e. the chemical state of the thin Cu films oxidized in air at different temperatures, X-ray photoemission spectroscopy (XPS) was employed. Figure 9(a) shows, the wide scan XPS spectra of thin Cu films of metallic and their oxides phases. The survey scans appear with the copper core level peaks of Cu2p (951.5 eV and 932.6 eV),
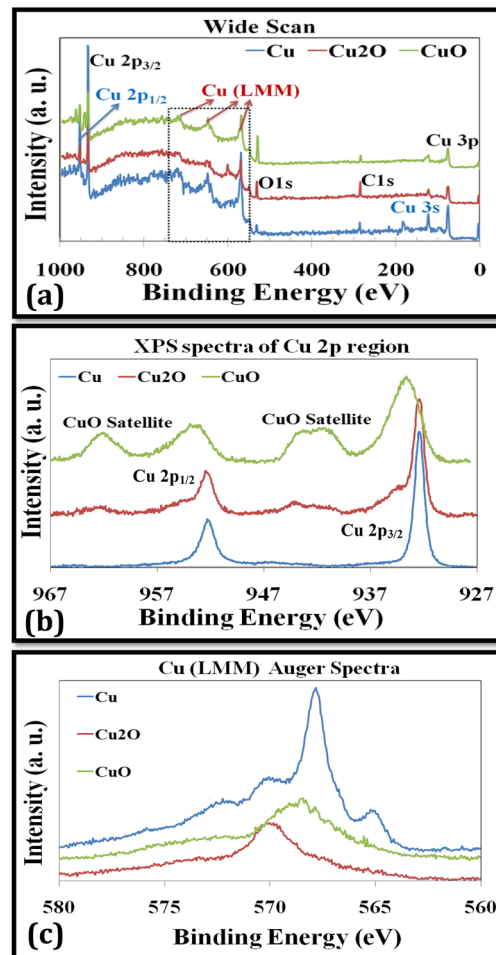

FIG. 9. XPS spectra of different Cu oxide films: (a) Survey Scan (b) Cu 2p core level and (c) LMM Auger spectra.

Cu3s (120.6 eV) and Cu3p (75.9 eV) and Cu LMM Auger peaks ($L_3M_{45}M_{45}$ at 568 eV, $L_3M_{23}M_{45}$ at 638 eV and $L_3M_{23}M_{23}$ at 715 eV), along with additional peaks of C1s (285 eV) and O1s (530.1 eV). Figures 9(b) and 9(c) present high resolution scans of Cu2p core level spectra and LMM Auger transmission lines, respectively. Three different chemical states of the Cu films (Cu, Cu_2O and CuO) are clearly marked and the relative shifts in peak positions of the binding energies are compared. Figure 9(b) shows high resolution Cu2p XPS data recorded for the copper thin film oxidized at 300 °C and 350 °C for 3 hours. It can be seen that Cu2p energy level of Cu and Cu_2O are composed of main characteristic doublet peaks correspond to $Cu2p_{1/2}$ and $Cu2p_{3/2}$, respectively, with a spin-orbit splitting of 19 eV. This is in good agreement with the values reported in the literature.[48,51,52] However, in case of CuO film, additional shake-up satellite peaks at 8 eV higher binding energy of the main Cu2p peak, originate from multiple excitations in copper oxides, are also found. These satellite peaks are known to be the characteristics of CuO phase.[48,51,52] $Cu2p_{3/2}$ binding energy peak of Cu^+ oxidation state of Cu_2O film appears at 932.65 eV which is very close to the metallic Cu^0 state of Cu film centered at 932.4 eV. However, a significant shift of about 1 eV towards higher BE side (933.65 eV) is found for Cu^{+2} oxidation state of CuO film. Well defined shake-up satellite peaks associated with the $Cu2p_{3/2}$ line also appeared. As there are no significant differences in the $Cu2p_{3/2}$ BE spectra for Cu and Cu_2O, it is difficult to determine the metallic Cu^0 phase within the Cu_2O oxide phase. To eliminate this possibility, we compare the Auger $L_3M_{45}M_{45}$ spectra of these films where a clear separation in the peak positions for metallic Cu (567.8 eV), Cu_2O (570.15 eV) and CuO (568.5 eV) has been noticed as shown in Fig. 9(c).[52,53] In XPS measurements the probing depth within the Cu oxide layer is expected to be only ~2 nm for incident photon energy of 1486.6 eV (Al Kα line).[48,53] This makes XPS highly surface sensitive. Even though, the satellite peaks corresponding to the Cu^{+2} oxidation state are not observed for Cu_2O film surface, which confirms the phase purity of the film. Therefore from all above findings (XRD, Raman spectroscopy and XPS) it can be concluded that within a particular range of oxidation temperature, a single oxide phase of crystalline Cu_2O film can be formed by thermal oxidation in an air ambient.

F. Effect of oxygen partial pressure

A special interest towards the influence of O_2 partial pressures to alter the activation temperature of the oxide phase is also tested. In case of oxidation under pure oxygen ambient at atmospheric pressure, the temperature window shifted significantly towards the lower value. For oxidation at 150 °C, a clear (111) diffraction peak of Cu_2O is observed in XRD along with the (111) and (200) diffraction peaks of Cu. This finding clearly indicates the crystalline Cu_2O formation already started at 150 °C which was not seen for the case of air oxidation process even at 200 °C (Figure S1 of the supplementary material). Similarly, oxidation at 250 °C under oxygen ambient results in CuO formation instead of Cu_2O formation in air oxidation (Figure S1 of the supplementary material). A similar temperature shift during oxidation of Cu films under various oxygen partial pressures has also been noticed by Khojjer *et. al.*[54] The lowering of the oxidation temperatures under oxygen ambient condition (leading to the successful formation of Cu oxide phases) has also been confirmed from XPS studies. In case of oxidation at 250 °C under oxygen ambient, XPS spectrum appears with the existence of a strong shake-up satellite peak of Cu2p, characteristic of the Cu^{+2} oxidation state of CuO. Moreover, oxidation of clean Cu films under low vacuum condition is also performed where the overall oxygen pressure was maintained much lower than the air ambient ($<10^{-3}$ mbar). A drastic shift of the oxidation temperature range towards higher value is expected here. Finally, it is also observed that the copper oxide films can completely be reduced to metallic copper by out gassing under ultra high vacuum condition (10^{-9} mbar) of the films at an elevated temperature above 700 °C (Figure S2 of the supplementary material). Wong *et. al* has also reported the effect of oxygen partial pressure towards the determination of the copper oxide phase during sputter growth of Cu_2O films.[12]

G. Effect of crystallographic orientations

It can be noticed from our earlier XRD patterns of Figures 3 and 4 that the oxidation process of the Cu films may also be influenced by the crystallographic orientations of the film surface. Figures 3(a) and 3(b) represent the evolution of Cu_2O phase with the oxidation time. Initially, the (111) diffraction

peak of Cu_2O starts to appear along with the Cu (111) and (200) diffraction lines. A clear growth preference of the (111) plane of Cu_2O over all other growth orientations is found. However, at the later stage towards the completion of the Cu_2O formation, (200) growth plane starts to dominate over the (111) growth plane of Cu_2O. On the other hand, no such preferential orientation is observed for the CuO growth. Figures 4(a) and 4(b) show both (-111) and (111) diffraction peaks start to appear from the beginning and maintain a relatively similar intensity profile throughout the formation of the CuO layer. These findings can be related to the initial crystalline orientation of the Cu grains where a dominating (111) plane is observed along with a weak (200) reflection. In addition, Cu and Cu_2O both exhibit a cubic crystal structure. The evolution of (200) diffraction peak at the later stage of Cu_2O formation may also be related to the relaxation of lattice stress of the oxide film through the rotational mismatch of the crystalline grains. Hence, a relatively faster oxidation may be expected at this stage due to the formation of additional grain boundaries.

IV. CONCLUSION

Thin films of single oxide phase of copper have successfully been grown on glass and silicon substrates by controlled thermal oxidation of vacuum deposited thin copper films. Sharp XRD patterns suggest the formation of highly crystalline films of copper oxides. Oxidation process of the Cu film is found to be highly sensitive to the diffusion kinetics. However, after sufficient duration of annealing (25 h), final oxide state of the Cu film is found to be determined by the oxidation temperature. This finding can be treated as thermodynamic equilibrium. Within the saturation limit, the completion of the oxidation process is mostly controlled by the diffusion kinetics (annealing duration) which further depends on the thickness of initial Cu layers. At a lower oxidation temperature range (250 °C – 320 °C) crystalline phase of Cu_2O is formed in air ambient condition whereas for higher oxidation temperature of 330 °C onwards, CuO phase starts to form. Within the range of diffusion limit, longer duration of annealing can lead to the completion of the transformation process of Cu_2O into the CuO phases. In case of single oxide phase of Cu_2O, faceted surface morphology of Cu_2O films, directed by its materialistic properties is observed in SEM images. In addition, Raman and photoemission spectroscopy also confirm the oxide phase purity for both cases. Finally, an optical band gap of about 2.2 eV for Cu_2O films has been observed, makes it a visible light active material suitable for the solar cell application.

Results of the present study indicate that nanostructured thin films of device quality Cu_2O and CuO can easily be achieved through this simple thermal oxidation method. Moreover, copper oxide based hetero-structures of Cu_2O/CuO can also be fabricated by following few simple steps as follows. The as-deposited copper thin film can initially be oxidized into CuO by annealing at a temperature above 330°C. In a subsequent step, metallic copper could be deposited on this system. Further annealing at a temperature between 250 °C – 320 °C in air can form the top Cu_2O layer on previously grown CuO film. This approach could be a promising move towards the recently reported copper oxide hetero-junctions based solar cell fabrication.[10] Alternatively, a Schottky barrier can also be formed by direct deposition (e.g. by evaporation) of copper or other metal on top of the oxidized Cu films.

SUPPLEMENTARY MATERIAL

See supplementary material for effect of oxygen partial pressure on determining the copper oxide phase as well as the oxidation temperature has been characterize using XRD and XPS. This material is available free of charge.

ACKNOWLEDGMENTS

[1] G. Zhou and J. C. Yang, Appl. Surf. Sci. **222**, 357 (2004).
[2] C. L. Chu, H. C. Lu, C. Y. Lo, C. Y. Lai, and Y. H. Wang, Physica B **404**, 4831 (2009).
[3] T. Schmidt, J. I. Flege, S. Gangopadhyay, T. Clausen, A. Locatelli, S. Heun, and J. Falta, Phys. Rev. Lett. **98**, 66104 (2007).
[4] S. Brittman, Y. Yoo, N. P. Dasgupta, S.-I. Kim, B. Kim, and P. Yang, Nano. Lett. **14**, 4665 (2014).
[5] Z. H. Lu and D. Grozea, Appl. Phys. Lett. **80**, 255 (2002).
[6] S. Lany, J. Phys.: Condens. Matt. **27**, 283203 (2015).
[7] J. D. Aiken and R. G. Finke, J. Mol. Catal. A Chem. **145**, 1 (1999).
[8] T. Guo, M. S. Yao, Y. H. Lin, and C.-W. Nan, Cryst. Eng. Comm. **17**, 3551 (2015).
[9] J. Ghijsen, L. H. Tjeng, J. van Elp, H. Eskes, J. Westerink, G. A. Sawatzky, and M. T. Czyzyk, Phys. Rev. B **38**, 11322 (1988).
[10] A. Mittiga, E. Salza, F. Sarto, M. Tucci, and R. Vasanthi, Appl. Phys. Lett. **88**, 163502 (2006).
[11] T. Minami, T. Miyata, K. Ihara, Y. Minamino, and S. Tsukada, Thin Solid Films **494**, 47 (2006).
[12] L. M. Wong, S. Y. Chiam, J. Q. Huang, S. J. Wang, J. S. Pan, and W. K. Chim, J. Appl. Phys. **108**, 033702 (2010).
[13] E. A. Souza, R. Landers, L. P. Cardoso, T. G. S. Cruz, M. H. Tabacniks, and A. Gorenstein, J. Power Sources **155**, 358 (2006).
[14] A. Paracchino, V. Laporte, K. Sivula, M. Grätzel, and E. Thimsen, Nat. Matter. **10**, 456 (2011).
[15] F. Oba, F. Ernst, Y. Yu, R. Liu, H. M. Kothari, and J. A. Switzer, J. Am. Ceram. Soc. **88**, 253 (2005).
[16] F. Marabelli, G. B. Parraviciny, and F. S. Drioli, Phys. Rev. B **52**, 1433 (1995).
[17] N. Serin, T. Serin, S. Horzum, and Y. Celik, Semicond. Sci. Technol. **20**, 398 (2005).
[18] H. G. Zhang, Q. Zhu, Y. Zhang, Y. Wang, L. Zhao, and B. Yu, Adv. Funct. Mater. **17**, 2766 (2007).
[19] R. A. Borzi, S. J. Stewart, R. C. Mercader, G. Punte, and F. Garcia, J. Magn. Magn. Mater. **226-230**, 1530 (2001).
[20] B. Balamurugan, B. R. Mehta, D. K. Avasthi, F. Singh, A. K. Arora, M. Rajalakshmi, G. Raghavan, A. K. Tyagi, and S. M. Sivaprasad, J. Appl. Phys. **92**, 3304 (2002).
[21] W. Wang, Z. Liu, Y. Liu, C. Xu, C. Zheng, and G. Wang, Appl. Phys. A **76**, 417 (2003).
[22] S. W. Lee, Y. S. Lee, J. Heo, S. C. Siah, D. Chua, R. E. Brandt, S. B. Kim, J. P. Mailoa, T. Buonassisi, and R. G. Gordon, Adv. Energy Mater. **4**, 1301916 (2014).
[23] Y. L. Liu, G. J. Yang, H. Zhang, Y. Q. Cheng, K. Q. Chen, Z. Y. Peng, and W. Chen, RSC Adv. **4**, 24363 (2014).
[24] L. Armelao, D. Barreca, M. Bertapelle, G. Bottaro, C. Sada, and E. Tondello, Thin Solid Films **442**, 48 (2003).
[25] T. Kosugi and S. Kaneko, J. Am. Ceram. Soc. **81**, 3117 (1998).
[26] M. Yang and J. J. Zhu, J. Cryst. Growth **256**, 134 (2003).
[27] S. Heiroth, R. Ghisleni, T. Lippert, J. Michler, and A. Wokaun, Acta Mater **59**, 2330 (2011).
[28] K. Amikura, T. Kimura, M. Hamada, N. Yokoyama, J. Miyazaki, and Y. Yamada, Appl. Surf. Sci **254**, 6976 (2008).
[29] S. B. Ogale, P. G. Bilurkar, N. Mate, S. M. Kanetkar, N. Parikh, and B. Patnaik, J. Appl. Phys. **72**, 3765 (1992).
[30] V. F. Drobny and D. L. Pulfrey, Thin Solid Films **61**, 89 (1979).
[31] S. Izhizuka, S. Kato, T. Maruyama, and K. Akimoto, Jpn. J. Appl. Phys. **40**, 2765 (2001).
[32] M. H. P. Reddy, A. Sreedhar, and S. Uthanna, Indian J. Phy **86**, 291 (2012).
[33] K. P. Muthe, J. C. Vyas, S. N. Narang, D. K. Aswal, S. K. Gupta, R. Pinto, G. P. Kothiyal, and S. B. Sabharwal, Thin Solids Films **324**, 37 (1998).
[34] A. Roos, T. Chibuye, and B. Karlson, Sol. Energy Mater **7**, 453 (1983).
[35] A. Fujinaka and A. A. Berezin, J. Appl. Phys. **54**, 3582 (1983).
[36] L. Wang and M. Tao, Electrochem. Solid-State Lett. **10**, H248 (2007).
[37] A. K. Mukhopadhyay, A. K. Chakraborty, A. P. Chatterjee, and S. K. Lahiri, Thin Solid Films **209**, 92 (1992).
[38] R. P. Wijesundera, Semicond. Sci. Technol. **25**, 045015 (2010).
[39] L. D. L. S. Valladares, D. H. Salinas, A. B. Dominguez, D. A. Najarro, S. I. Khondaker, T. Mitrelias, C. H. W. Barnes, J. A. Aguiar, and Y. Majima, Thin Solid Films **250**, 6368 (2012).
[40] H. Derin and K. Kantarli, Appl. Phys. A **75**, 391 (2002).
[41] G. Papadimitropoulos, N. Voirdas, V. Em Vamvakas, and D. Davazoglou, J. Phys.: Conference Series **10**, 182 (2005).
[42] A. O. Musa, T. Akomolafe, and M. J. Carter, Solar Energy Materials and Solar Cells **51**, 305 (1998).
[43] V. Figueiredo, E. Elangovan, G. Goncalves, P. Barqunha, L. Pereira, N. Franco, E. Alves, R. Martins, and E. Fortunato, Appl. Surf. Sci. **254**, 3949 (2008).
[44] S. Choudhary, J. V. N. Sarma, and S. Gangopadhyay, AIP Conf. Proc. **1724**, 020116-1 (2015).
[45] B. D. Hall, D. Zanchet, and D. Ugarte, J. Appl. Crystallography **33**(Part 6) (2000).
[46] W. L. Yu, Y. Z. Lin, X. W. Zhu, Z. G. Hu, M. J. Han, S. S. Cai, L. L. Chen, and H. H. Shao, J. Appl. Phys. **117**, 045701 (2015).
[47] J. F. Xu, W. Ji, Z. X. Shen, W. S. Li, S. H. Tang, X. R. Ye *et al.*, J. Raman Spectrosc. **30**, 431 (1999).
[48] F. A. Akgul, G. Akgul, N. Yildirim, H. E. Unalan, and R. Turan, Mat. Chem. Phys. **147**, 987 (2014).
[49] P. Kubelka and F. Munk, Z Tech Phys **12**, 593 (1931).
[50] J. Liang, N. Kishi, T. Soga, T. Jimbo, and M. Ahmed, Thin Solid Film **520**, 2679 (2012).
[51] D. Tahir and S. Tougaard, J. Phys. Condens. Matter **24**, 175002 (2012).
[52] D. Barreca, A. Gasparotto, and E. Tondello, Surf. Sci. Spec. **40**, 41 (2007).
[53] C. Powell and A. Jablonski, *NIST Inelastic Mean Free Path Database* (National Institute of Standards and Technology, Gaithersburg, MD, 2000).
[54] K. Khojier, H. Savaloni, and Z. Sadeghi, J. Theor. Appl. Phys. **8**(1), 116 (2014).